Altered reactivity to threatening stimuli in *Drosophila* models of Parkinson's disease, revealed by a trial-based assay

Márton Kajtor[1], Viktor A. Billes[2,3], Bálint Király[1,4], Hannah Stabb[1], Katalin Sviatkó[1,5], Eszter Ujvári[1], Diána Balázsfi[1], Sophie E. Seidenbecher[6], Duda Kvitsiani[7], Tibor Vellai[2,3], Balázs Hangya[1,*]

1 Lendület Laboratory of Systems Neuroscience, Institute of Experimental Medicine, H-1083 Budapest, Hungary

2 Department of Genetics, Eötvös Loránd University, H-1117 Budapest, Hungary

3 ELKH-ELTE Genetic Research Group, H-1117 Budapest, Hungary

4 Department of Biological Physics, Eötvös Loránd University, H-1117 Budapest, Hungary

5 János Szentágothai Doctoral School of Neurosciences, Semmelweis University, H-1085 Budapest, Hungary

6 University of Technology Nuremberg, Nuremberg, Germany

7 Department of Molecular Biology and Genetics, Danish Research Institute of Translational Neuroscience, Aarhus University, Aarhus, Denmark

* Correspondence: Balázs Hangya, hangya.balazs@koki.hu

Abstract

The fruit fly *Drosophila melanogaster* emerges as an affordable, genetically tractable model of behavior and brain diseases. However, despite the surprising level of evolutionary conservation from flies to humans, significant genetic and circuit-level differences hinder the interpretability of fruit fly models for human disease. Therefore, to facilitate fly-to-human translation with more direct behavior-level comparison, we surveyed the rarely-exploited, rich behavioral repertoire of fruit flies with genetic alterations relevant to Parkinson's disease (PD). Flies displayed variable behaviors, including freezing, slowing and running, in response to predator-mimicking passing shadows used as threatening stimuli in a single-animal trial-based assay. We found that the expression of human mutant Parkin in flies resulted in reduced walking speed and decreased reactivity to passing shadows. Flies with dopamine receptor mutations showed similar alterations, consistent with the motor and cognitive deficits typical in humans

with PD. However, *Drosophila* overexpressing the human form of α-synuclein manifested in only moderate phenotypical alterations, suggesting that other fruit fly models may be favored in PD research. We also found age-dependent trends in behavioral choice across the fly lifespan, while dopamine receptor mutant flies maintained their decreased general reactivity throughout all age groups. Our data demonstrate that single-trial behavioral analysis can reveal subtle behavioral changes in mutant flies that can be used to further our understanding of disease pathomechanisms and help gauge the validity of genetic *Drosophila* models of neurodegeneration.

Introduction

Parkinson's disease (PD) affects over 6 million people worldwide, representing the second most common neurodegenerative disease. PD is slowly progressing and typically leads to years of aggravating disability, thereby placing a huge burden on families, health care systems and the society, measured in hundreds of billions of dollars annually (Olesen et al., 2012; Obeso et al., 2017; Przedborski, 2017; Bloem et al., 2021). Therefore, a hitherto elusive disease-modifying therapy is of prominent priority, envisioned to be fueled by research into basic mechanisms of the disease.

Patients with PD display a diverse set of motor and non-motor symptoms with an underlying progressive loss of midbrain dopaminergic neurons (Schapira, 2009; Schapira et al., 2017; Bloem et al., 2021), mechanisms of which are widely studied in animal models of the disease. Primate models offer the advantage of more direct translatability but are restricted to hard-to-handle neurotoxin approaches and do not promise fast progress. Unlike the genetic mouse models of Alzheimer's disease, most of the successful rodent models of PD are also toxin-based, making it difficult to exploit and further our understanding of the genetic bases of the disease (Cannon and Greenamyre, 2010; Bové and Perier, 2012; Breger and Fuzzati Armentero, 2019). This left a niche for the genetically tractable, affordable fruit flies as genetic models of PD (Feany and Bender, 2000; Guo, 2012; Hewitt and Whitworth, 2017), building on the homologies between the vertebrate basal ganglia and the fruit fly central complex (Strausfeld and Hirth, 2013). However, substantial genetic, anatomical, physiological, and behavioral discrepancies between insects and mammals call for better validation methods of fruit fly models for human disease. To address this, here we used a single-animal trial-based behavioral assay that facilitates fine-grained assessment of phenotypical behavioral changes in fruit flies with mutations relevant to understanding human PD.

Genes linked to familial forms of PD may serve as an ideal basis for genetic disease models. Notably, mutations in the *PARK2* gene, which encodes the Parkin protein involved in maintaining mitochondrial integrity, are associated with autosomal-recessive forms of PD (Guo, 2012). Parkin loss-of-function mutant flies were found to have advanced mitochondrial aging, structural mitochondrial damage and a consequential selective loss of dopaminergic neurons (Cackovic et al., 2018), leading to motor deficits assessed by a climbing assay (Chambers et al., 2013; Cackovic et al., 2018), as well as non-motor PD phenotypes including memory deficits (Julienne et al., 2017). Mutations in the *SNCA* gene of α-Synuclein (α-Syn) are also associated with familiar forms of PD (Polymeropoulos et al., 1997) and α-Syn has been shown to accumulate in Lewy-bodies and Lewy-neurites (Spillantini et al., 1997). α-Syn proteins have been found in the pre-synaptic terminals in humans and mice (Kahle et al., 2000) and are thought to be involved in dopamine (DA) synthesis under physiological conditions by reducing tyrosine hydroxylase activity (Perez et al., 2002). Expression of human α-Syn in flies has been proposed as a genetic model of PD, showing age-dependent loss of dopaminergic neurons and locomotor dysfunction in a climbing assay (Feany and Bender, 2000; Haywood and Staveley, 2006). However, other studies found normal locomotion and dopaminergic cell counts in these flies, casting doubts on the validity of this model (Pesah et al., 2005; Nagoshi, 2018).

Despite the observed homology between mammalian and fruit fly DA systems in motor control and the establishment of *Drosophila* PD models based on human genetic information derived from familial PD patients, the role of *Drosophila* DA receptors in locomotor control is not well characterized. Nevertheless, it has been demonstrated that the D1-like DA receptor mediates ethanol-induced locomotion in the ellipsoid body (Kong et al., 2010). Furthermore, *Dop1R1* has been shown to be involved in turning behavior for goal-directed locomotion (Kottler et al., 2019) and startle-induced negative geotaxis (Sun et al., 2018). To shed light on the possible roles of DA receptors in threat-induced motor behaviors, we tested the behavioral responses of three dopamine receptor (*Dop1R1*, *Dop1R2* and *DopEcR*) insertion mutant lines to predator-mimicking passing shadows and compared them to established fruit fly PD models with partially known locomotor deficits.

We found that flies expressing the R275W mutant allele of human Parkin ('Parkin flies') showed slower average locomotion speed, which, in contrast, was not characteristic of flies expressing the A53T mutant allele of the human *SNCA* gene ('α-Syn flies'). Parkin flies also showed less frequent freezing and generally less behavioral reactivity to passing shadows compared to controls, whereas α-Syn flies showed increased durations of stopping after the stimuli. Dopamine receptor mutant flies showed reduced speed and less

behavioral reactivity similar to Parkin flies. *Dop1R1* mutant flies exhibited more pronounced behavioral alterations than the other two receptor mutants in most of the parameters tested. These data demonstrate that mutations in DA receptor genes lead to specific patterns of behavioral deficits in *Drosophila*; hence, these dopamine receptor paralogs may have different functions in behavioral control. The modest phenotype of A53T α-Syn compared to Parkin flies suggests that the latter should be favored as a genetic model of human PD, at least with respect to the motor deficits examined in this study. We further propose that single-trial analyses such as those we present here help us gain a better understanding of the behavioral changes in fruit fly models of PD and are strong tools for validating *Drosophila* models of human diseases.

Results

A single-animal trial-based assay to test behavioral responses to predator-mimicking passing shadows

We designed a behavioral apparatus to examine the responses of individual flies to predator-mimicking passing shadows. To do this, we designed a transparent plexiglass arena (Fig. 1a), featuring 13 tunnels (53 mm x 5 mm) for simultaneous tracking of 13 individual flies. The height of the tunnels (1 mm) was designed to allow free walking in two dimensions but prevent jumps and flight. To simulate predatory threat, we created passing 'shadows' (Fig. 1a, right; see Methods) with a sliding red screen presented on a 10.1-inch display placed on the top of the arena. A high frame-rate camera was placed under the arena (Fig. 1a, left), allowing us to simultaneously record the movement of the animals and the shadows. All 13 tunnels housed a single fly in each session, enabling the collection of single-animal data from 13 flies in parallel. The locomotion of individual flies was tracked by custom software developed using the Bonsai visual programming environment (Fig. S1, see Methods). We recorded 40-minute-long sessions, consisting of 40 trials of 2-second-long shadow presentations separated by pseudorandom inter-trial-intervals to prevent the animals from learning temporal expectations of the shadow presentations (Fig. 1b).

Fruit flies exhibit a rich behavioral repertoire upon threatening stimuli, including freezing (or stopping) and various escape behaviors such as jumping, slow or fast take-off and running, modulated by walking speed at the time of the threatening stimulus (Zacarias et al., 2018). To study these behaviors, we calculated the speed and acceleration of fruit flies based on the tracked x-y position of their center of mass (Fig. 2a) and aligned these signals to the presentations of the shadow stimuli. To identify separate response types to the threating stimuli, we applied hierarchical clustering on these stimulus-aligned speed

traces (see Methods). This analysis consistently revealed three main stereotypical behavioral responses across flies in addition to the trials where no significant response was evoked (Fig. 2b). Since jumping and flying was not possible in the arena, fruit flies were restricted to choose among freezing, slowing (also observed in (Zacarias et al., 2018)) and running. While this clustering approach was sufficient to reveal response types qualitatively, cluster boundaries were sensitive to genotype-specific differences across groups of flies (Király and Hangya, 2022). Therefore, for rigorous group comparisons, we determined exact definitions of each response type based on fly speed and acceleration (Fig. 2c). Reactions were considered robust if the absolute value of the acceleration reached 200 mm/s^2; otherwise, the trial was classified as a 'no reaction' trial. We considered the reaction as a 'stop' if the animal was moving before shadow presentation and its speed decreased to zero in the first second relative to the shadow presentation. If fly speed decreased to a non-zero value, the trial was defined as 'slow down', and if the fly accelerated after the shadow presentation, the trial was classified as 'speed up' (see also Methods).

Parkinson's model and dopamine receptor mutant fruit flies showed reduced walking speed and decreased reactivity to threatening stimuli

To generate PD fly models, we expressed the mutant human Parkin (275W) and α-Syn (A53T) coding transgenes (*UAS-Parkin-275W* and *UAS-α-Syn-A53T*, respectively), applying the UAS-Gal4 system (Duffy, 2002). Transgenes were driven by *Ddc-Gal4* inducing the expression of the correspondent human mutant proteins in dopaminergic and serotoninergic fly neurons. Parkin and α-Syn flies were compared to control animals from the same genetic background without mutant transgenes (*Ddc-Gal4* animals were crossed with *iso* w^{1118}, the examined F1 generation flies are referred to as *iso* w^{1118} Fig. 3) or mutants overexpressing GFP (Fig. S2). The same level of eye pigmentation and vision of the compared genotypes was achieved by the prior replacement of the *w** mutant first chromosome of the applied *Ddc-Gal4* stock for that of the wild-type . The dopamine receptor mutant groups were compared to their parental strains without the mutations (y^1 w^{67c23} served as control for *Dop1R1* and *Dop1R2* and w^{1118} for *DopEcR*; Fig. 3).

To test whether mutant flies showed differences in overall locomotion independent of the threatening stimuli, we analyzed average fly speed in the 200 ms time windows before stimulus presentation. We found that Parkin flies showed reduced mean speed compared to controls which expressed the Gal4 driver alone (24.96% reduction, $p = 6.55 \times 10^{-6}$, Mann-Whitney U-test; Fig. 3a, top), while α-Syn flies did not show significant reduction ($p = 0.799$, Mann–Whitney U-test). We observed similar changes in dopamine

receptor mutant flies, where the *Dop1R1* and *DopEcR* defective lines showed a robust mean speed decrease compared to the control groups (*Dop1R1*, 19.68% decrease compared to $y^1\ w^{67c2}$, p = 0.0016; *DopEcR*, 32.97% decrease compared to w^{1118}, p = 0.0034; Fig. 3a, bottom), while the *Dop1R2* mutant flies only showed a non-significant speed decrease (21.73% compared to $y^1\ w^{67c23}$, p = 0.1009, Mann–Whitney U-test).

Next, we tested whether mutant flies showed a difference in their reaction to threatening stimuli. We found that PD model flies showed line-specific alterations in their freezing behavior. Parkin flies froze after stimuli less frequently, stopping in 37.72% of trials compared to the 43.48% observed in the *iso* w^{1118} animals (p = 0.0043, Mann Whitney U-test; Fig. 3b, top). However, in the stop trials, they showed normal duration of pauses in locomotion (p = 0.8018 compared to *iso* w^{1118}, Mann Whitney U-test; Fig. 3c, top). In contrast, α-Syn flies showed an unchanged stopping frequency when compared to controls (p = 0.0768 compared to *iso* w^{1118}, Mann-Whitney U-test), but their stop durations showed a large increase (116.98% increase compared to *iso* w^{1118}, $p = 2.18 \times 10^{-11}$, Mann-Whitney U-test). Interestingly, in contrast to PD model flies, dopamine receptor mutant flies did not show significant differences in their freezing behavior relative to controls (stop proportion: *Dop1R1*, p = 0.0631 compared to $y^1\ w^{67c23}$; *Dop1R2*, p = 0.1838 compared to $y^1\ w^{67c23}$; *DopEcR*, p = 0.1445 compared to w^{1118}; Mann-Whitney U-test; Fig. 3b, bottom; stop duration: *Dop1R1*, p = 0.893 compared to $y^1\ w^{67c23}$; *Dop1R2*, p = 0.154 compared to $y^1\ w^{67c23}$; *DopEcR*, p = 0.3576 compared to w^{1118}; Mann-Whitney U-test; Fig. 3c, bottom).

α-Syn flies showed a reduced aptitude to increase their speed, or 'run', upon encountering threatening stimuli (26.67% decrease compared to *iso* w^{1118}, $p = 8.4 \times 10^{-6}$, Mann-Whitney U-test; Fig. 3d, top). Similar results were found in *Dop1R1* (25% decrease compared to $y^1\ w^{67c23}$, p = 0.0122; Mann-Whitney U-test; Fig. 3d, bottom) and *Dop1R2* (41.67% decrease compared to $y^1\ w^{67c23}$, p = 0.0024, Mann-Whitney U-test), but not in *DopEcR* mutant flies (compared to w^{1118}, p = 0.6598, Mann-Whitney U-test). Frequency of slowing, i.e., reducing their speed without freezing in a full stop, was moderately decreased in Parkin (14.38% decrease compared to *iso* w^{1118}, p = 0.0723, Mann-Whitney U-test; Fig. 3e, top) and *DopEcR* mutant flies (15.28% decrease compared to w^{1118}, p = 0.020, Mann-Whitney U-test; Fig. 3e, bottom).

Overall, all mutations tested resulted in decreased reactivity to threatening stimuli, confirmed by a significant increase in the proportion of trials where no reactions were detected (Fig. 3f). This effect was significant for Parkin flies (30% increase compared to *iso* w^{1118}, p = 0.0043, Mann-Whitney U-test), as well as for *Dop1R1* (50% increase compared to $y^1\ w^{67c23}$, p = 0.0173, Mann-Whitney U-test) and *DopEcR* mutant flies (50% increase compared to w^{1118}, p = 0.0167, Mann-Whitney U-test), but not for α-Syn (α-Syn vs. *iso*

179 w^{1118}, p = 0.151, Mann-Whitney U-test) and *Dop1R2* mutant flies (*Dop1R2* vs. $y^1 w^{67c23}$, p = 0.1903, Mann-
180 Whitney U-test).

181

182 **Reaction to threatening stimuli depends on fly walking speed**

183 It has been shown that fruit flies may exhibit a different choice of escape behavior based on their
184 momentary speed when encountering the threat (Zacarias et al., 2018). Therefore, we tested whether
185 mutations in genes relevant to PD caused a change in this speed - behavioral response relationship. We
186 calculated the probability of stopping, slowing, speeding up and no reaction as a function of speed for all
187 mutants, as well as the ratio of each response type conditioned on walking speed at the time of shadow
188 presentations (Fig. 4a-b). These analyses confirmed that 'running' and 'no reaction' was most likely at
189 slow (< 5 mm/s) or zero walking speeds, while slowing down was more frequent as the walking speed
190 increased. Freezing was most frequently observed in the 5-13 mm/s speed range. We did not observe
191 significant difference between groups in their speed - behavioral response relationship for any of the
192 response types (stops, p = 0.4226; slow down, p = 0.6025; speed up, p = 0.9074; no reaction p = 0.4692;
193 two-way ANOVA genotype × speed interaction).

194 Since the distribution of the expression of various escape behaviors depended on walking speed, which
195 was also different across the mutant lines tested (Fig. 3), we asked whether the difference in baseline
196 speed could explain the observed differences in behavioral reactions. Therefore, we performed
197 simulations where reaction probabilities were based on the baseline walking speed distribution of each
198 mutant line to test whether behavioral responses could be predicted based on speed alone (Fig. S3). In
199 most of the groups we found a significant difference between the predicted and the measured response
200 type distributions, suggesting a role for other behavioral differences among the mutant lines beyond the
201 baseline speed differences (Parkin, p = 0.0487; α-Syn, p < 0.000001; *Dop1R1*, p = 0.332; *Dop1R2*, p =
202 0.006157; *DopEcR*, p = 0.003901, chi-square test).

203

204 **Changes in escape behavior from the first to the fourth week of life**

205 The age of *Drosophilae* may have a significant influence on their responses to threatening stimuli. To test
206 this, we examined control and dopamine receptor mutant flies (w^{1118}, $y^1 w^{67c23}$, *Dop1R1*, *Dop1R2*, *DopEcR*)
207 in 5 age groups: from 1-day-old to 4-week-old (Fig. 5; Fig. S4). The animals were kept under conditions

that accelerated their aging (29°C and 70% humidity). Our data showed that the behavior of 1-day-old flies was significantly different from all other age groups. One-day-old flies stopped significantly more often, and the frequency of stopping gradually decreased with age in all groups (two-way ANOVA, age, $p = 1.87 \times 10^{-20}$, $f = 26.11$; genotype, $p = 1.3 \times 10^{-29}$, $f = 38.42$; genotype × age, $p = 3.18 \times 10^{-6}$, $f = 3.54$; 1-day-old vs. 1-week-old, $p = 1.33 \times 10^{-5}$; 1-week-old vs. 2-week-old, $p = 0.017$, 2-week-old vs. 3-week-old, $p = 0.63$; 3-week-old vs. 4-week-old, $p = 0.098$, Tukey's test for post hoc analysis). In contrast, the probability of slowing down showed a substantial increase from 1-day-old to 1-week-old animals, and then remained unchanged until the 4th week (two-way ANOVA, age, $p = 9.11 \times 10^{-15}$, $f = 18.72$; genotype, $p = 1.4 \times 10^{-21}$, $f = 27.59$; genotype × age, $p = 0.0028$, $f = 2.291$; 1-day-old vs. 1-week-old, 1-week-old vs. 2-week-old, $p = 2.56 \times 10^{-8}$; $p = 1$; 2-week-old vs. 3-week-old, $p = 0.13$; 3-week-old vs. 4-week-old, $p = 0.093$; Tukey's test for post hoc analysis). The probability of speeding up showed a similar trend, except that the 4-week-old animals showed a significant decrease compared to 3-week-old flies (two-way ANOVA, age, $p = 2.48 \times 10^{-15}$, $f = 19.44$; genotype, $p = 2.28 \times 10^{-44}$, $f = 59.48$; genotype × age, $p = 1.1 \times 10^{-7}$, $f = 4.12$; 1-day-old vs 1-week-old, $p = 9.92 \times 10^{-9}$; 1-week-old vs. 2-week-old, $p = 0.79$; 2-week-old vs. 3-week-old, $p = 0.75$; 3-week-old vs. 4-week-old, $p = 0.024$; Tukey's test for post hoc analysis). Thus, different types of escape reactions showed similar trends across the fly lifespan, while dopamine receptor mutant flies maintained their decreased general reactivity throughout all age groups.

Discussion

We tested *Drosophila* mutant strains relevant for Parkinson's disease in a single-trial single-animal behavioral assay. Our tests revealed strain-specific behavioral alterations in flies' reactions to predator-mimicking passing shadows, serving as proof of principle demonstration of the viability of single-trial approaches in *Drosophila*, a method widely used in mammalian studies. Specifically, we found reduced walking speed, decreased freezing frequency and decreased overall reactivity in Parkin flies. In contrast, α-Syn flies merely showed an increased freezing duration without a concomitant change in freezing frequency, suggesting that Parkin flies better recapitulate some behavioral features of human PD progression. *Dop1R* mutant flies resembled Parkin flies in their decreased walking speed and decreased reactivity to the threatening stimuli. The distribution of the behavioral response fruit flies chose to execute depended on their speed at the time of stimuli, and this speed - behavioral response relationship was robust across the tested genotypes. Nevertheless, differences in walking speed alone did not explain

238 the strain-specific behavioral alterations. Age-dependence of the behavioral choice was also found to be
239 stereotypic across the tested genotypes.

240 Recent studies increasingly recognize the importance of investigating subtle changes in fly behavior to
241 better understand the manifestations of locomotor and other disorders (Geissmann et al., 2017; Zacarias
242 et al., 2018; Seidenbecher et al., 2020). Along these lines, Aggarwal and colleagues introduced an
243 automated climbing assay for fruit flies and revealed subtle motor deficits in different mutant strains
244 (Aggarwal et al., 2019). We expanded the scope of these studies by examining a diverse behavioral
245 repertoire of *Drosophila* in response to threatening stimuli. The diversity of freeze vs. flee responses of
246 fruit flies, including different durations of stopping as well as running, were accurately described by
247 Zacarias et al. (Zacarias et al., 2018), where they also identified DNp09 neurons as important controllers
248 of running and freezing responses. We built on this behavioral characterization for our definitions of fly
249 reactions to predator-mimicking stimuli.

250 Mutations in the *PARK2* gene lead to impaired ubiquitination and a consequential mitochondrial
251 dysfunction (Guo, 2010, 2012), and early-onset PD in human patients. This led to the widespread use of
252 Parkin flies as a genetic model pf PD (Guo, 2010; Chambers et al., 2013; Aggarwal et al., 2019). Of note,
253 flies that lack Parkin display a significant degeneration of dopaminergic neurons (Whitworth et al., 2005).
254 We found similarities between Parkin and *Dop1R* mutant flies in their altered responses to predator-
255 mimicking passing shadows: reduced walking speed and decreased overall reactivity, suggesting that the
256 lack of dopamine action through *Dop1R* may be one of the common pathways underlying motor deficits.
257 This is in line with a recent study demonstrating impaired startle-induced geotaxis and locomotor
258 reactivity in *Dop1R* mutant flies (Sun et al., 2018), similar to what had been shown for Parkin flies
259 (Aggarwal et al., 2019), and a demonstration of dopaminergic control over walking speed (Marquis and
260 Wilson, 2022). In contrast, flies expressing human α-syn showed moderate changes in motor behavior
261 except for a marked prolongation of freezing duration upon threating stimuli. This is in accordance with
262 studies suggesting that α-syn misexpression is not fully penetrant under some conditions (Pesah et al.,
263 2005; Nagoshi, 2018), and calls for the use of other genetic *Drosophila* models, including Parkin flies, in
264 studying the pathophysics of human PD.

265 The dopamine/ecdysteroid receptor *DopEcR* is a G-protein-coupled dual receptor for dopamine and the
266 steroid hormone ecdysone. It has been proposed that the *DopEcR* may serve as an integrative hub for
267 dopamine-mediated actions and stress responses in fruit flies (Petruccelli et al., 2020). We found that
268 *DopEcR* mutant flies showed decreased mean walking speed, decreased probability of slowing down and

decreased overall behavioral reactivity in response to predator-mimicking passing shadows. This pattern of alterations was largely similar to those observed in Parkin and *Dop1R* mutant flies, suggesting that the *DopEcR* may convey similar dopamine-mediated functions as *DopR1* at least in those motor aspects tested in the present study. A recent work demonstrated that serotonin also modulates both walking speed and startle response in flies, suggesting a complex neuromodulatory control over *Drosophila* motor behavior (Howard et al., 2019).

In humans, degeneration of midbrain dopaminergic neurons has been found as a direct cause of PD symptoms and DA supplementation with its precursor levodopa has been one of the most successful therapeutic approaches to date. The fruit fly and mammalian DA systems show a number of homologies which are thought to serve as a good basis for *Drosophila* PD models (Feany and Bender, 2000; Hewitt and Whitworth, 2017). Specifically, a deep-running evolutional conservation has been revealed between the arthropod central complex and the vertebrate basal ganglia, where GABAergic and dopaminergic neurons play key roles in motor control in both phylae (Strausfeld and Hirth, 2013). Clusters of fly dopaminergic neurons that project to the ellipsoid body, the fan-shaped body and the lateral accessory lobes are thought to share homologies with the striatum-projecting dopaminergic neurons of the substantia nigra in mammals. Both the fruit fly central complex and vertebrate basal ganglia mediate a range of functions from motor control and sensorimotor integration to action selection and decision making to motivation (Strauss, 2002; Claridge-Chang et al., 2009; Kong et al., 2010) and learning (McCurdy et al., 2021; Zolin et al., 2021; Fisher et al., 2022; Qiao et al., 2022; Taisz and Jefferis, 2022; Yamada et al., 2023). It has been found that fruit flies lacking the DA-synthetizing tyrosine hydroxylase enzyme in the central nervous system show reduced activity and locomotor deficit that worsen with age, and also exhibit marked impairments in associative learning based on both appetitive and aversive reinforcement (Riemensperger et al., 2011). This is in line with mammalian studies emphasizing the role of the dopaminergic nigrostriatal pathway in controlling goal-directed action (Eban-Rothschild et al., 2016), reinforcement learning (Schultz et al., 1997; Lak et al., 2014), and more recently, conveying aversive information (Menegas et al., 2015, 2018). Our findings are consistent with the apparent homologies across fruit fly and mammalian dopaminergic systems and suggest that a more in-depth investigation of specific behavioral changes and underlying dopamine-related dysfunctions may yield translatable results. We also observed age-related changes in motor behavior in response to threatening stimuli, particularly in 4-week-old flies, which may parallel the age-dependent worsening of PD symptoms in humans.

Acknowledgements

We thank the Anne Von Phillipsborn lab, DANDRITE, Aarhus University for the kind gift of the DA receptor mutant lines. Most of the *Drosophila* stocks were obtained from the Bloomington Drosophila Stock Center (NIH P40OD018537). We thank the FENS-Kavli Network of Excellence for fruitful discussions. B.H. was supported by the Eotvos Lorand Research Network. T.V. was supported by the grants OTKA (Hungarian Scientific Research Fund) K132439 and VEKOP (VEKOP-2.3.2-16-2017-00014), and by the ELKH/MTA-ELTE Genetics Research Group (01062).

Data and code availability

All analysis functions are available at https://github.com/hangyabalazs/Drosophila-behavior-analysis. All data are available at https://figshare.com/s/40539ee040a269bf05e5.

Methods

Animals

We used 2-weeks-old *Drosophila melanogaster* (both males and females) raised at 24°C and 60% humidity in a natural light-dark cycle for experiments presented in Figures 1-4. For age-group comparisons (Fig.5.), fruit flies aged 1, 7, 14, 21 and 28 days were used. These flies were raised at 29°C and 70% humidity to accelerate aging.

Two sets of mutant groups were used for behavioral comparison. In the first set of animals we used *w*; UAS-Parkin-R275W* (created in the laboratory of Kah-Leong Lim, Neurodegeneration Research Laboratory, National Neuroscience Institute, Singapore)(Wang et al., 2007; Kovács et al., 2017) and *w*; UAS-alpha-Syn-A53T* (BDSC 8148) from the Eotvos Lorand University, with y^1, v^1; *UAS-GFP* (BDSC 35786) and *+; P{Ddc-GAL4.L}4.36* (modified version of BDSC 7009, the original first chromosome w^{1118} has been replaced to w^+ in this study) as controls. For the second set of animals we used *Dop1R1*, *Dop1R2* and *DopEcR* mutant flies kindly donated by the Anne Von Phillipsborn lab, DANDRITE, Aarhus University and y^1 *w*; Mi{MIC}Dop1R1*^{MI04437} (BDSC 43773), y^1 *w*; Mi{MIC}Dop1R2*^{MI08664} (BDSC 51098), and w^{1118}; *PBac{PB}DopEcR*^{c02142}*/TM6B, Tb*^{1} (BDSC 10847) with w^{1118} (BDSC 5905) y^1 and y^1 w^{67c23} (BDSC 6599) as controls from the Bloomington stock centre. Table 1. shows the number of recorded flies for the age group comparisons, and Table 2. shows the number of recorded flies for comparing the mutant groups.

	Dop1R1	*Dop1R2*	*DopEcR*	w^{1118}	y^{1} w^{67c23}
1-day-old	35	36	36	35	41
1-week-old	36	54	36	36	36
2-week-old	36	36	36	36	30
3-week-old	35	35	29	36	36
4-week-old	30	36	34	30	30

Table 1. Number of recorded flies for the age group comparisons.

2-week-old	No. of flies
Dop1R1	45
Dop1R2	47
DopEcR	35
w^{1118}	46
y^{1}, w^{67c23}	40
Parkin	78
α-Syn	69
iso w^{1118}	92
+GFP	65

Table 2. Number of recorded flies for comparing the mutant groups.

Arena

We designed an arena made of four layers of plexiglass and metal that formed 13 tunnels (Fig. 1a). Each tunnel was 52mm x 5mm × 1mm, in which individual flies were able to move freely in two dimensions but could not fly. The bottom layer was a standard transparent plexiglass layer. The second layer contained the tunnel walls made of metal to prevent horizontal spread of light. The third layer was the top of the tunnels, made of transparent plexiglass, which could slide above the tunnel. It also contained a small hole on the side, where the flies could be inserted into the tunnel through a pipette. The fourth layer was a metal cover designed with cut-outs that matched the shape and position of the tunnels to prevent flies in the neighboring tunnels from detecting the shadow before it reached their position.

Movement tracking

Flies were tracked by using a FLIR Camera (FLIR Blackfly S USB3 FLIR Systems, Wilsonville, OR, US) placed under the arena (Fig. 1a). The frame rate was set to 100 frames/second to allow the detection of position with high temporal resolution. The recorded images were processed by Bonsai (2.5.2) tracking software (Lopes et al., 2015), using customized Bonsai code. The code extracts each tunnel areas separately from the image and detects flies by selecting the biggest and darkest pixel object in the tunnel area in real time. Fly position coordinates were calculated from the centroid. The software stored x-y position coordinates

346 along with their timestamps in csv files, which were later processed in Matlab R2016a (Mathworks, Natick,
347 MA, US).

348 **Predator-mimicking shadow stimuli**

349 A 10.1-inch screen (HannStar HSD101PWW1-A00,) was placed on the top of the arena. The screen
350 presented a yellow background. We implemented 'shadow' stimuli in red color, as these stimuli were
351 suggested to be perceived by fruit flies as dark shadows and also enabled continuous tracking of the
352 animals (Sharkey et al., 2020). The red color screen represented a large enough contrast change to evoke
353 escape behaviors of flies, but also provided sufficient brightness to enable continuous motion tracking. A
354 passing shadow stimulus was chosen, as it was affecting all tunnels simultaneously. To mimic an
355 approaching shadow, a red screen slid in from the side, stayed on for 2 seconds, then slid out. The shadow
356 stimuli were separated by pseudorandomized inter-trial intervals with an approximately exponential
357 distribution with a mean of 52.2 seconds, preventing flies from anticipating the next shadow stimulus.

358 **Identification of behavioral response types to the threatening stimuli**

359 Animal speed was calculated as a function of time in a -200 ms to 1000 ms window around each shadow
360 stimulus in 10 ms time bins. These speed functions were normalized by subtracting the average speed in
361 the 200 ms window before the shadow presentation to reveal stimulus induced absolute instantaneous
362 speed changes. Principal component analysis (PCA) was used to reduce dimensionality of the normalized
363 speed functions in the 1 s interval following shadow presentation in a way that the variance between trials
364 is maximally preserved in the low-dimensional representation. Agglomerative hierarchical clustering was
365 performed in the space spanned by the first three principal components to identify trials with distinct
366 characteristic response types.

367 **Behavior detection**

368 After identifying the four most frequently observed animal responses to shadow presentations, we
369 algorithmically defined them based on the speed and acceleration thresholds. First, we examined the
370 speed of the animal in the 200 ms time window before the shadow (v_{pre}); stopping/freezing or slowing
371 down was only possible if the fly had been moving, defined by $v_{pre} > 0$ mm/s. Second, we examined the
372 acceleration (a_{post}) in the 1 s interval following the shadow using a 100 ms moving average window to
373 characterize the flies' response. Reactions were considered robust if the absolute value of the acceleration
374 reached 200 mm/s^2. A trial was characterized as a 'stop' trial, if the average v_{pre} was above 0 mm/s, the
375 fly's first reaction was deceleration, and 0 mm/s speed was reached before accelerating again. If the first

reaction was deceleration but 0 mm/s speed was not reached, the trial was classified as a 'slow down' trial. In 'speed up' trials, the first response following the shadow was acceleration. If the absolute value of a_{post} did not reach the 200 mm/s^2 threshold during the 1 s interval following the shadow, the trial was labeled as a 'no reaction' trial.

Data analysis and statistics

Data analysis was performed in Matlab R2016a (Mathworks, Natick, MA, US) using custom-written code. Statistical comparison between groups of flies was performed by two-sided Mann-Whitney U-test. Exact p values are reported in the Results section. The effect of movement speed on the distribution of behavioral response types was tested using Monte Carlo simulation (Fig.S3). First, we calculated the probability of each response type at different speed values from the grand average of all trails of every animal. Then we simulated behavior of virtual flies by drawing random velocity values from the velocity distribution of each genotype and then randomly selecting a reaction based on the reaction probabilities associated with the drawn velocity. Finally, we calculated reaction probabilities for the virtual flies and compared it with real data from animals of the same genotype. Differences were statistically tested by Chi-squared test.

Figure Legends

Fig. 1. Behavioral apparatus and experimental design.

a, Top left, schematic of the experimental setup. Top right, schematic of the fly arena. Bottom left, photograph of the experimental setup. Bottom right, a photograph of the fly arena. **b,** Timeline of a session showing the shadow presentations in red over the yellow background.

Fig. 2. Behavioral characterization of the escape behavior repertoire of individual fruit flies.

a, Schematic for calculating speed and acceleration based on tracked position coordinates. **b,** Four characteristic escape behaviors categorized by PCA for an example session of a control fly (w1118; from left; stop, slow down, speed up, no reaction). Top, color-coded heatmaps indicating the walking speed of the fly (blue, low speed; yellow, high speed), aligned to shadow presentations (orange line). Bottom, average moving speed triggered on the shadow presentations (orange line). **c,** Threshold-based classification of behavioral responses (from left, stop, slow down, speed up, no reaction). Top, single-trial example for each response type. Time intervals for calculating the average speed before the shadow presentation (orange) as well as the speed and acceleration after the shadow presentation (green) are

marked. Threshold values for each response type are displayed above the graphs. Bottom, average walking speed across the trials from all session of w^{1118} flies, sorted by the type of behavioral response. Line and errorshade show mean ± SE.

Fig. 3. Parkinson's model and dopamine receptor mutant fruit flies showed reduced walking speed and decreased reactivity to threatening stimuli.

a, Distribution of the mean speed measured in the time window [-0.2, 0] seconds relative to shadow presentation for the different mutant groups. Top, Parkin flies showed reduced mean speed compared to controls (Parkin vs. *iso* w^{1118}; $p = 6.55 \times 10^{-6}$, Mann–Whitney U-test). Bottom, *Dop1R1* and *DopEcR* mutant flies showed reduced mean speed compared to controls (y^1w^{67c23} and w^{1118} respectively; p = 0.0016, p = 0.0034; Mann-Whitney U-test). **b,** Distribution of the proportion of stop trials in different mutant groups. Parkin flies showed a reduced tendency for stopping compared to *iso* w^{1118} (p = 0.0043, Mann Whitney U test). **c,** Distribution of stop duration in different mutant groups. α-Syn flies showed increased stop durations compared to *iso* w^{1118} ($p = 2.18 \times 10^{-11}$, Mann-Whitney U-test). **d,** Distribution of the proportion of speed up trials in different mutant groups. Top, α-Syn flies showed a reduced tendency to speed up compared to their controls ($p = 8.4 \times 10^{-6}$, Mann-Whitney U-test). Bottom, *Dop1R1* and *Dop1R2* mutant flies also showed a significantly reduced tendency to speed up compared to their controls (p = 0.0122 and p = 0.0024, respectively; Mann-Whitney U-test). **e,** Distribution of the proportion of slow down trials in different mutant groups. Bottom, *DopEcR* showed a 15.04% decrease compared to w^{1118} (p = 0.020, Mann-Whitney U-test). **f,** Distribution of the proportion of 'no reaction' trials in different mutant groups. Top, Parkin mutants showed reduced reactivity compared to *iso* w^{1118} controls (p = 0.0043, Mann-Whitney U-test). Bottom, *Dop1R1* and *DopEcR* mutants also showed reduced reactivity compared to y^1w^{67c23} and w^{1118} controls, respectively (p = 0.0173 and p = 0.0167, respectively; Mann-Whitney U-test). Box-whisker plots show median, interquartile range and non-outlier range. *, $p < 0.05$; **, $p < 0.01$; ***, $p < 0.001$. Exact genotypes: *iso* w^{1118}: *+; +; Ddc-Gal4/+*. Parkin: *+; +; Ddc-Gal4/UAS-Parkin-R275W*. α-Syn: *+; +; Ddc-Gal4/UAS-α-Syn-A53T*. y^1 w^{67c23}: y^1 w^{67c23}. *Dop1R*: y^1 *w*; Mi{MIC}Dop1R1*^{MI04437}. *Dop1R2*: y^1 *w*; Mi{MIC}Dop1R2*^{MI08664}. *DopEcR*: w^{1118}*; PBac{PB}DopEcR*^{c02142}*/TM6B, Tb*^{1}.

Fig. 4. Reaction to threatening stimuli depends on fly walking speed.

a, Probability of a given response type as a function of average fly speed before the shadow presentation (200 ms pre-stimulus time window). From left, stop, slow down, speed up and no reaction trials are quantified. Top, Parkin and α-Syn flies. Bottom, *Dop1R1*, *Dop1R2* and *DopEcR* mutant flies. **b,** Proportion

of a given response type as a function of average fly speed before the shadow presentation. Top, Parkin and α-Syn flies. Bottom, *Dop1R1*, *Dop1R2* and *DopEcR* mutant flies. Exact genotypes: *iso* w^{1118}: *+; +; Ddc-Gal4/+.* Parkin: *+; +; Ddc-Gal4/UAS-Parkin-R275W*. α-Syn: *+; +; Ddc-Gal4/UAS-α-Syn-A53T*. y^1 w^{67c23}: y^1 w^{67c23}. *Dop1R*: y^1 *w*; Mi{MIC}Dop1R1*^{MI04437}. *Dop1R2*: y^1 *w*; Mi{MIC}Dop1R2*^{MI08664}. *DopEcR*: w^{1118}*; PBac{PB}DopEcR*^{c02142}*/TM6B, Tb*^{1}.

Fig. 5. Changes in escape behavior from the first to the fourth week of life

Proportion of responses as a function of age for different groups of mutants and controls. From left to right, stop, slow down, speed up and no reaction trials are quantified. Lines and errorshades show mean and standard error. Exact genotypes: *iso* w^{1118}: *+; +; Ddc-Gal4/+.* Parkin: *+; +; Ddc-Gal4/UAS-Parkin-R275W*. α-Syn: *+; +; Ddc-Gal4/UAS-α-Syn-A53T*. y^1 w^{67c23}: y^1 w^{67c23}. *Dop1R*: y^1 *w*; Mi{MIC}Dop1R1*^{MI04437}. *Dop1R2*: y^1 *w*; Mi{MIC}Dop1R2*^{MI08664}. *DopEcR*: w^{1118}*; PBac{PB}DopEcR*^{c02142}*/TM6B, Tb*^{1}.

Supplementary Figure Legends

Fig. S1. Picture of the arena from the camera view

The 13 tunnels of the arena from the camera view with the tracking lines showing that the animals can move in 2 dimnesions. The tracking line color indicates time, with dark blue and red marking the beginning and the end of the tracking, respectively.

Fig. S2. Parkin and α-Syn fly group escape reaction compared to GFP mutant flies

a, Distribution of the mean speed measured in the 0.2 second before shadow presentation for Parkin, α-Syn and +GFP mutant groups. Parkin and α-Syn flies showed reduced mean speed compared to +GFP controls (Parkin vs. +GFP, $p = 1.58 \times 10^{-11}$; α-Syn vs. +GFP, $p = 2.85 \times 10^{-4}$; Mann-Whitney U-test). **b,** Distribution of the proportion of stop trials in different mutant groups. Parkin flies showed reduced tendency for stopping compared to the +GFP group (Parkin vs. +GFP, $p = 7.1 \times 10^{-5}$; α-Syn vs. +GFP, p = 0.67; Mann-Whitney U-test). **c,** Distribution of stop duration in different mutant groups. α-Syn flies showed increased stop durations compared to GFP (Parkin vs. +GFP, p = 0.17; α-Syn vs. +GFP, $p = 3.98 \times 10^{-10}$; Mann-Whitney U-test). **d,** Distribution of the proportion of speed up trials in different mutant groups. Both Parkin and α-Syn flies showed a reduced tendency to speed up compared to +GFP controls (Parkin vs. +GFP, $p = 8.3 \times 10^{-5}$; α-Syn vs. +GFP, $p = 1.96 \times 10^{-12}$; Mann-Whitney U-test). **e**, Distribution of the proportion of slow down trials in different mutant groups. Parkin flies showed a reduced tendency to slow down compared to +GFP controls (Parkin vs. +GFP, p = 0.044; α-Syn vs. +GFP, p = 0.465; Mann-Whitney U-test). **f**, Distribution of the proportion of 'no reaction' trials in different mutant groups. Both

Parkin and α-Syn flies showed reduced reactivity compared to +GFP controls (Parkin vs. +GFP, $p = 9.4 \times 10^{-13}$; α-Syn vs. +GFP, $p = 1{,}3 \times 10^{-8}$; Mann-Whitney U-test). *, $p < 0.05$; **, $p < 0.01$; ***, $p < 0.001$. Exact genotypes: *iso* w^{1118}: *+; +; Ddc-Gal4/+.* Parkin: *+; +; Ddc-Gal4/UAS-Parkin-R275W*. α-Syn: *+; +; Ddc-Gal4/UAS-α-Syn-A53T*.

Fig. S3. Differences in walking speed do not explain different escape behaviors

Real and simulated proportion of response types are shown for the mutant groups tested. For the simulations, random velocity values were drawn from the velocity distribution of each genotype and then a response type was randomly selected based on the response type distributions associated with the drawn velocity. Bar plots show the proportion of response types color-coded. For each mutant group, the right bar shows the measured proportion of escape responses, while the left bar shows the simulated distribution. We found significant differences between the real and simulated distributions for the following groups: Parkin ($p = 0.0487$), α-Syn ($p < 0.000001$), *Dop1R2* ($p = 0.006157$) and *DopEcR* ($p = 0.003901$). We found no significant differences for the *Dop1R1* group ($p = 0.332$; Chi-square test for all the statistics). *, $p < 0.05$; **, $p < 0.01$; ***, $p < 0.001$. Exact genotypes: *iso* w^{1118}: *+; +; Ddc-Gal4/+.* Parkin: *+; +; Ddc-Gal4/UAS-Parkin-R275W*. α-Syn: *+; +; Ddc-Gal4/UAS-α-Syn-A53T*. y^1 w^{67c23}: y^1 w^{67c23}. *Dop1R*: y^1 *w*; Mi{MIC}Dop1R1*^{MI04437}. *Dop1R2*: y^1 *w*; Mi{MIC}Dop1R2*^{MI08664}. *DopEcR*: w^{1118}; *PBac{PB}DopEcR*^{c02142}*/TM6B,* Tb^1.

Fig. S4. Changes in escape behavior from the first to the fourth week of life

a, Average walking speed as a function of age for different groups of controls (left) and mutants (right). Lines and errorshades show mean and standard error. Mean speed showed significant differenceis among age groups (two-way ANOVA, age, $f = 41.38$, $p = 9.39 \times 10^{-32}$; genotype, $f = 42.19$, $p = 2.46 \times 10^{-32}$; genotype × age, $f = 4.36$, $p = 2.667 \times 10^{-8}$;Tukey's post hoc test: 1 day old vs. 1 week old, $p = 9.92 \times 10^{-9}$; 1 week old vs. 2 weeks old, $p = 7.34 \times 10^{-7}$; 2 weeks old vs. 3 weeks old, $p = 0.085$; 3 weeks old vs. 4 weeks old, $p = 0.0043$). **b,** Stop duration as a function of age for different groups of controls (left) and mutants (right). We found that age did not effect the duration of stops (two-way ANOVA, age, $f = 0.85$, $p = 0.49$; genotype, $f = 0.91$, $p = 0.46$; genotype × age, $f = 2.53$, $p = 0.0008$; Tukey's post hoc test: 1 day old vs. 1 week old, $p = 0.98$; 1 week old vs. 2 weeks old, $p = 0.992$; 2 weeks old vs. 3 weeks old, $p = 0.578$; 3 weeks old vs. 4 weeks old, $p = 0.9759$). Lines and errorshades show mean and standard error.

References

495 Aggarwal A, Reichert H, VijayRaghavan K (2019) A locomotor assay reveals deficits in heterozygous
496 Parkinson's disease model and proprioceptive mutants in adult Drosophila. Proc Natl Acad Sci U S A
497 116:24830–24839.

498 Bloem BR, Okun MS, Klein C (2021) Parkinson's disease. Lancet 397:2284–2303.

499 Bové J, Perier C (2012) Neurotoxin-based models of Parkinson's disease. Neuroscience 211:51–76.

500 Breger LS, Fuzzati Armentero MT (2019) Genetically engineered animal models of Parkinson's disease:
501 From worm to rodent. Eur J Neurosci 49:533–560.

502 Cackovic J, Gutierrez-Luke S, Call GB, Juba A, O'Brien S, Jun CH, Buhlman LM (2018) Vulnerable parkin
503 loss-of-function Drosophila dopaminergic neurons have advanced mitochondrial aging,
504 mitochondrial network loss and transiently reduced autophagosome recruitment. Front Cell
505 Neurosci 12:1–14.

506 Cannon JR, Greenamyre JT (2010) Neurotoxic in vivo models of Parkinson's disease. In: Progress in Brain
507 Research, pp 17–33. Elsevier B.V.

508 Chambers RP, Call GB, Meyer D, Smith J, Techau JA, Pearman K, Buhlman LM (2013) Nicotine increases
509 lifespan and rescues olfactory and motor deficits in a Drosophila model of Parkinson's disease.
510 Behav Brain Res 253:95–102.

511 Claridge-Chang A, Roorda RD, Vrontou E, Sjulson L, Li H, Hirsh J, Miesenböck G (2009) Writing Memories
512 with Light-Addressable Reinforcement Circuitry. Cell 139:405–415.

513 Duffy JB (2002) GAL4 system indrosophila: A fly geneticist's swiss army knife. genesis 34:1–15.

514 Eban-Rothschild A, Rothschild G, Giardino WJ, Jones JR, De Lecea L (2016) VTA dopaminergic neurons
515 regulate ethologically relevant sleep-wake behaviors. Nat Neurosci 19:1356–1366.

516 Feany MB, Bender WW (2000) A Drosophila model of Parkinson's disease. Nature 404:394–398.

517 Fisher YE, Marquis M, D'Alessandro I, Wilson RI (2022) Dopamine promotes head direction plasticity
518 during orienting movements. Nature 612:316–322.

519 Geissmann Q, Garcia Rodriguez L, Beckwith EJ, French AS, Jamasb AR, Gilestro GF (2017) Ethoscopes: An
520 open platform for high-throughput ethomics. PLOS Biol 15:e2003026.

521 Guo M (2010) What have we learned from Drosophila models of Parkinson's disease? In: Progress in

522 Brain Research, pp 2–16. Elsevier B.V.

523 Guo M (2012) Drosophila as a model to study mitochondrial dysfunction in Parkinson's disease. Cold
524 Spring Harb Perspect Med 2:1–18.

525 Haywood AFM, Staveley BE (2006) Mutant α-synuclein-induced degeneration is reduced by parkin in a
526 fly model of Parkinson's disease. Genome 49:505–510.

527 Hewitt VL, Whitworth AJ (2017) Mechanisms of Parkinson's Disease. In: Current Topics in Developmental
528 Biology, 1st ed., pp 173–200. Elsevier Inc.

529 Howard CE, Chen C-L, Tabachnik T, Hormigo R, Ramdya P, Mann RS (2019) Serotonergic Modulation of
530 Walking in Drosophila. Curr Biol 29:4218-4230.e8.

531 Julienne H, Buhl E, Leslie DS, Hodge JJL (2017) Drosophila PINK1 and parkin loss-of-function mutants
532 display a range of non-motor Parkinson's disease phenotypes. Neurobiol Dis 104:15–23.

533 Kahle PJ, Neumann M, Ozmen L, Müller V, Jacobsen H, Schindzielorz A, Okochi M, Leimer U, Van Der
534 Putten H, Probst A, Kremmer E, Kretzschmar HA, Haass C (2000) Subcellular localization of wild-
535 type and Parkinson's disease-associated mutant α-synuclein in human and transgenic mouse brain.
536 J Neurosci 20:6365–6373.

537 Király B, Hangya B (2022) Navigating the Statistical Minefield of Model Selection and Clustering in
538 Neuroscience. eNeuro 9.

539 Kong EC, Woo K, Li H, Lebestky T, Mayer N, Sniffen MR, Heberlein U, Bainton RJ, Hirsh J, Wolf FW (2010)
540 A pair of dopamine neurons target the D1-like dopamine receptor dopr in the central complex to
541 promote ethanol-stimulated locomotion in drosophila. PLoS One 5.

542 Kottler B, Faville R, Bridi JC, Hirth F (2019) Inverse Control of Turning Behavior by Dopamine D1 Receptor
543 Signaling in Columnar and Ring Neurons of the Central Complex in Drosophila. Curr Biol 29:567-
544 577.e6.

545 Kovács T et al. (2017) The small molecule AUTEN-99 (autophagy enhancer-99) prevents the progression
546 of neurodegenerative symptoms. Sci Rep 7:42014.

547 Lak A, Stauffer WR, Schultz W (2014) Dopamine prediction error responses integrate subjective value
548 from different reward dimensions. Proc Natl Acad Sci U S A 111:2343–2348.

549 Lopes G, Bonacchi N, Frazão J, Neto JP, Atallah B V., Soares S, Moreira L, Matias S, Itskov PM, Correia PA,
550 Medina RE, Calcaterra L, Dreosti E, Paton JJ, Kampff AR (2015) Bonsai: an event-based framework
551 for processing and controlling data streams. Front Neuroinform 9:7.

552 Marquis M, Wilson RI (2022) Locomotor and olfactory responses in dopamine neurons of the Drosophila
553 superior-lateral brain. Curr Biol 32:5406-5414.e5.

554 McCurdy LY, Sareen P, Davoudian PA, Nitabach MN (2021) Dopaminergic mechanism underlying reward-
555 encoding of punishment omission during reversal learning in Drosophila. Nat Commun 12:1115.

556 Menegas W, Akiti K, Amo R, Uchida N, Watabe-Uchida M (2018) Dopamine neurons projecting to the
557 posterior striatum reinforce avoidance of threatening stimuli. Nat Neurosci 21:1421–1430.

558 Menegas W, Bergan JF, Ogawa SK, Isogai Y, Venkataraju KU, Osten P, Uchida N, Watabe-Uchida M
559 (2015) Dopamine neurons projecting to the posterior striatum form an anatomically distinct
560 subclass. Elife 4:1–30.

561 Nagoshi E (2018) Drosophila Models of Sporadic Parkinson's Disease. Int J Mol Sci 19:3343.

562 Obeso JA et al. (2017) Past, present, and future of Parkinson's disease: A special essay on the 200th
563 Anniversary of the Shaking Palsy. Mov Disord 32:1264–1310.

564 Olesen J, Gustavsson a., Svensson M, Wittchen HU, Jönsson B (2012) The economic cost of brain
565 disorders in Europe. Eur J Neurol 19:155–162.

566 Perez RG, Waymire JC, Lin E, Liu JJ, Guo F, Zigmond MJ (2002) A Role for α-Synuclein in the Regulation of
567 Dopamine Biosynthesis. J Neurosci 22:3090–3099.

568 Pesah Y, Burgess H, Middlebrooks B, Ronningen K, Prosser J, Tirunagaru V, Zysk J, Mardon G (2005)
569 Whole-mount analysis reveals normal numbers of dopaminergic neurons following misexpression
570 of?-Synuclein inDrosophila. genesis 41:154–159.

571 Petruccelli E, Lark A, Mrkvicka JA, Kitamoto T (2020) Significance of DopEcR, a G-protein coupled
572 dopamine/ecdysteroid receptor, in physiological and behavioral response to stressors. J
573 Neurogenet 34:55–68.

574 Polymeropoulos MH et al. (1997) Mutation in the α-synuclein gene identified in families with Parkinson's
575 disease. Science (80-) 276:2045–2047.

576 Przedborski S (2017) The two-century journey of Parkinson disease research. Nat Rev Neurosci 18:251–
577 259.

578 Qiao J, Yang S, Geng H, Yung W-H, Ke Y (2022) Input-timing-dependent plasticity at incoming synapses of
579 the mushroom body facilitates olfactory learning in Drosophila. Curr Biol 32:4869-4880.e4.

580 Riemensperger T, Isabel G, Coulom H, Neuser K, Seugnet L, Kume K, Iché-Torres M, Cassar M, Strauss R,
581 Preat T, Hirsh J, Birman S (2011) Behavioral consequences of dopamine deficiency in the
582 Drosophila central nervous system. Proc Natl Acad Sci U S A 108:834–839.

583 Schapira AHV (2009) Neurobiology and treatment of Parkinson's disease. Trends Pharmacol Sci 30:41–
584 47.

585 Schapira AHV, Chaudhuri KR, Jenner P (2017) Non-motor features of Parkinson disease. Nat Rev
586 Neurosci 18:435–450.

587 Schultz W, Dayan P, Montague PR (1997) A neural substrate of prediction and reward. Science
588 275:1593–1599.

589 Seidenbecher SE, Sanders JI, von Philipsborn AC, Kvitsiani D (2020) Reward foraging task and model-
590 based analysis reveal how fruit flies learn value of available options Skoulakis EMC, ed. PLoS One
591 15:e0239616.

592 Sharkey CR, Blanco J, Leibowitz MM, Pinto-Benito D, Wardill TJ (2020) The spectral sensitivity of
593 Drosophila photoreceptors. Sci Rep.

594 Spillantini MG, Schmidt ML, Lee VM-Y, Trojanowski JQ, Jakes R, Goedert M (1997) α-Synuclein in Lewy
595 bodies. Nature 388:839–840.

596 Strausfeld NJ, Hirth F (2013) Deep homology of arthropod central complex and vertebrate basal ganglia.
597 Science (80-) 340:157–161.

598 Strauss R (2002) The central complex and the genetic dissection of locomotor behaviour. Curr Opin
599 Neurobiol 12:633–638.

600 Sun J, Xu AQ, Giraud J, Poppinga H, Riemensperger T, Fiala A, Birman S (2018) Neural control of startle-
601 induced locomotion by the mushroom bodies and associated neurons in drosophila. Front Syst
602 Neurosci 12:1–18.

603 Taisz I, Jefferis GSXE (2022) Speed of learning depends on turning. Nature 612:216–217.

604 Wang C, Lu R, Ouyang X, Ho MWL, Chia W, Yu F, Lim K-L (2007) Drosophila Overexpressing Parkin R275W
605 Mutant Exhibits Dopaminergic Neuron Degeneration and Mitochondrial Abnormalities. J Neurosci
606 27:8563–8570.

607 Whitworth AJ, Theodore DA, Greene JC, Beneš H, Wes PD, Pallanck LJ (2005) Increased glutathione S -
608 transferase activity rescues dopaminergic neuron loss in a Drosophila model of Parkinson's disease.
609 Proc Natl Acad Sci 102:8024–8029.

610 Yamada D, Bushey D, Li F, Hibbard KL, Sammons M, Funke J, Litwin-Kumar A, Hige T, Aso Y (2023)
611 Hierarchical architecture of dopaminergic circuits enables second-order conditioning in Drosophila.
612 Elife 12:1–30.

613 Zacarias R, Namiki S, Card GM, Vasconcelos ML, Moita MA (2018) Speed dependent descending control
614 of freezing behavior in Drosophila melanogaster. Nat Commun 9:1–11.

615 Zolin A, Cohn R, Pang R, Siliciano AF, Fairhall AL, Ruta V (2021) Context-dependent representations of
616 movement in Drosophila dopaminergic reinforcement pathways. Nat Neurosci 24:1555–1566.

617

618

619 **Figures**

620 **Figure 1**

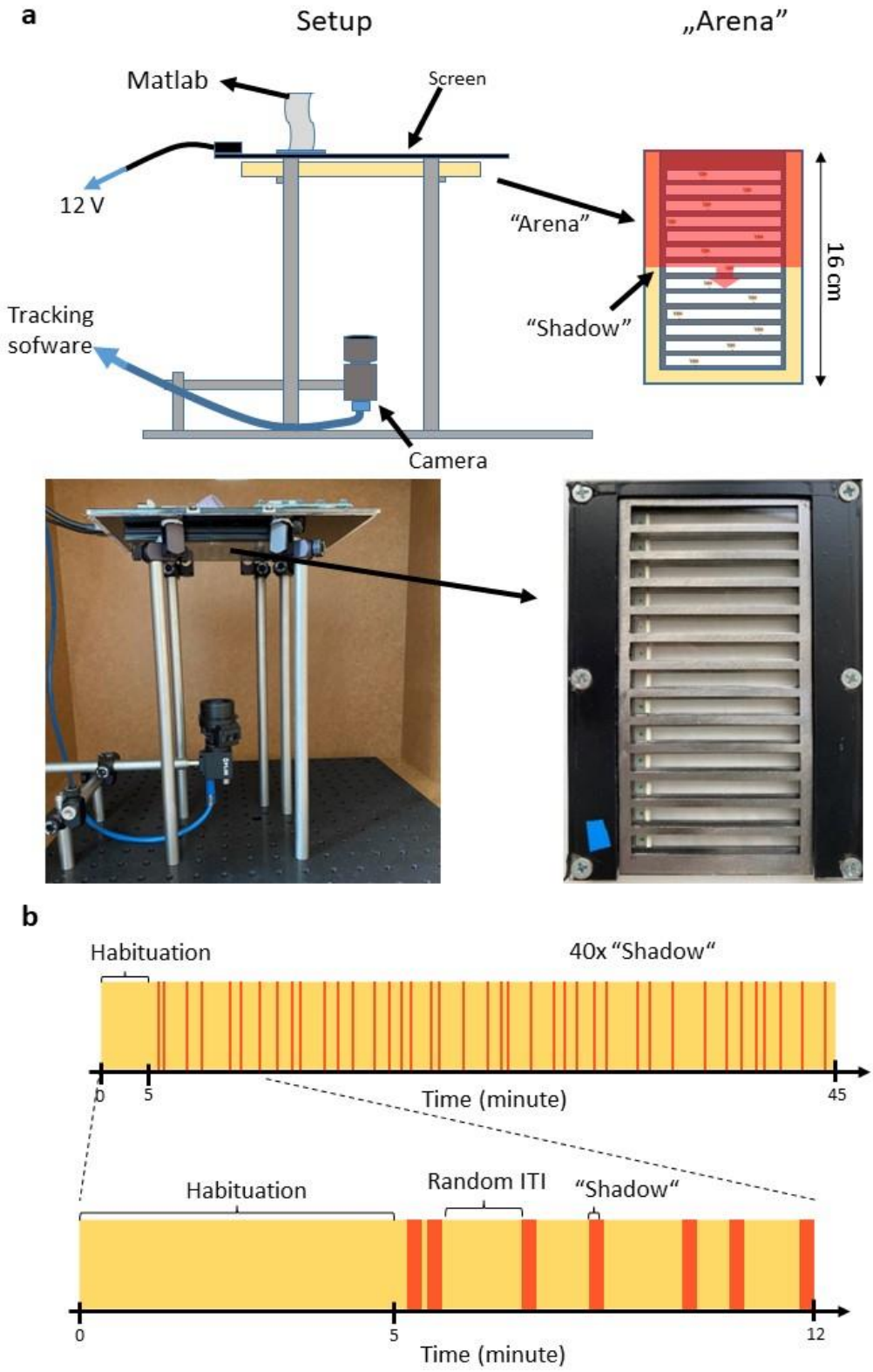

621

Figure 2

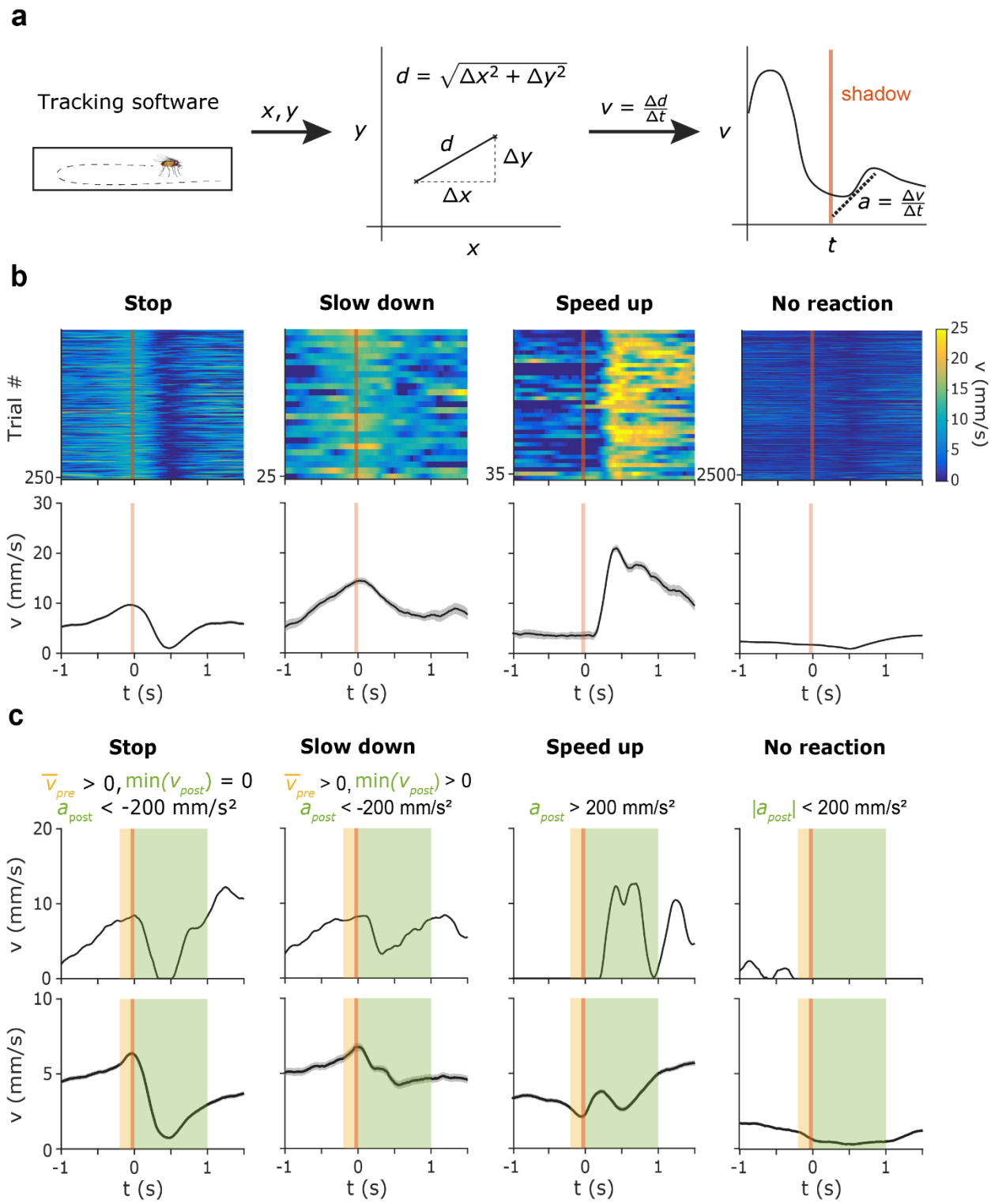
a
Tracking software
x, y
y
x
d = √(Δx² + Δy²)
d
Δy
Δx
v = Δd/Δt
v
t
shadow
a = Δv/Δt
b
Stop
Slow down
Speed up
No reaction
Trial #
250
25
35
2500
v (mm/s)
t (s)
c
Stop
Slow down
Speed up
No reaction
v̄pre > 0, min(vpost) = 0
apost < -200 mm/s²
v̄pre > 0, min(vpost) > 0
apost < -200 mm/s²
apost > 200 mm/s²
|apost| < 200 mm/s²
v (mm/s)
t (s)

Figure 3

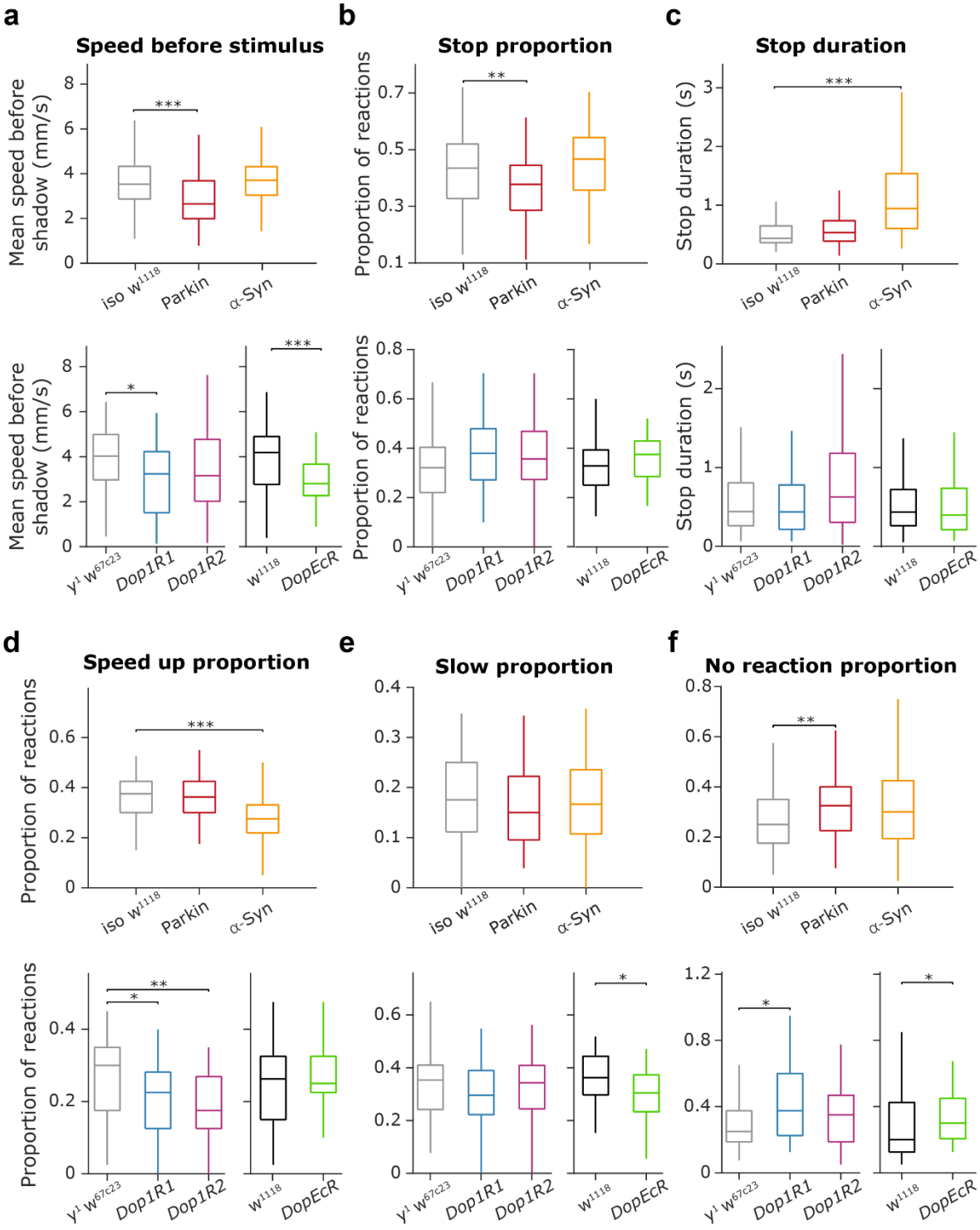
a
Speed before stimulus
Mean speed before shadow (mm/s)
iso w1118
Parkin
α-Syn
y1 w67c23
Dop1R1
Dop1R2
w1118
DopEcR
b
Stop proportion
Proportion of reactions
c
Stop duration
Stop duration (s)
d
Speed up proportion
e
Slow proportion
f
No reaction proportion

628 **Figure 4**

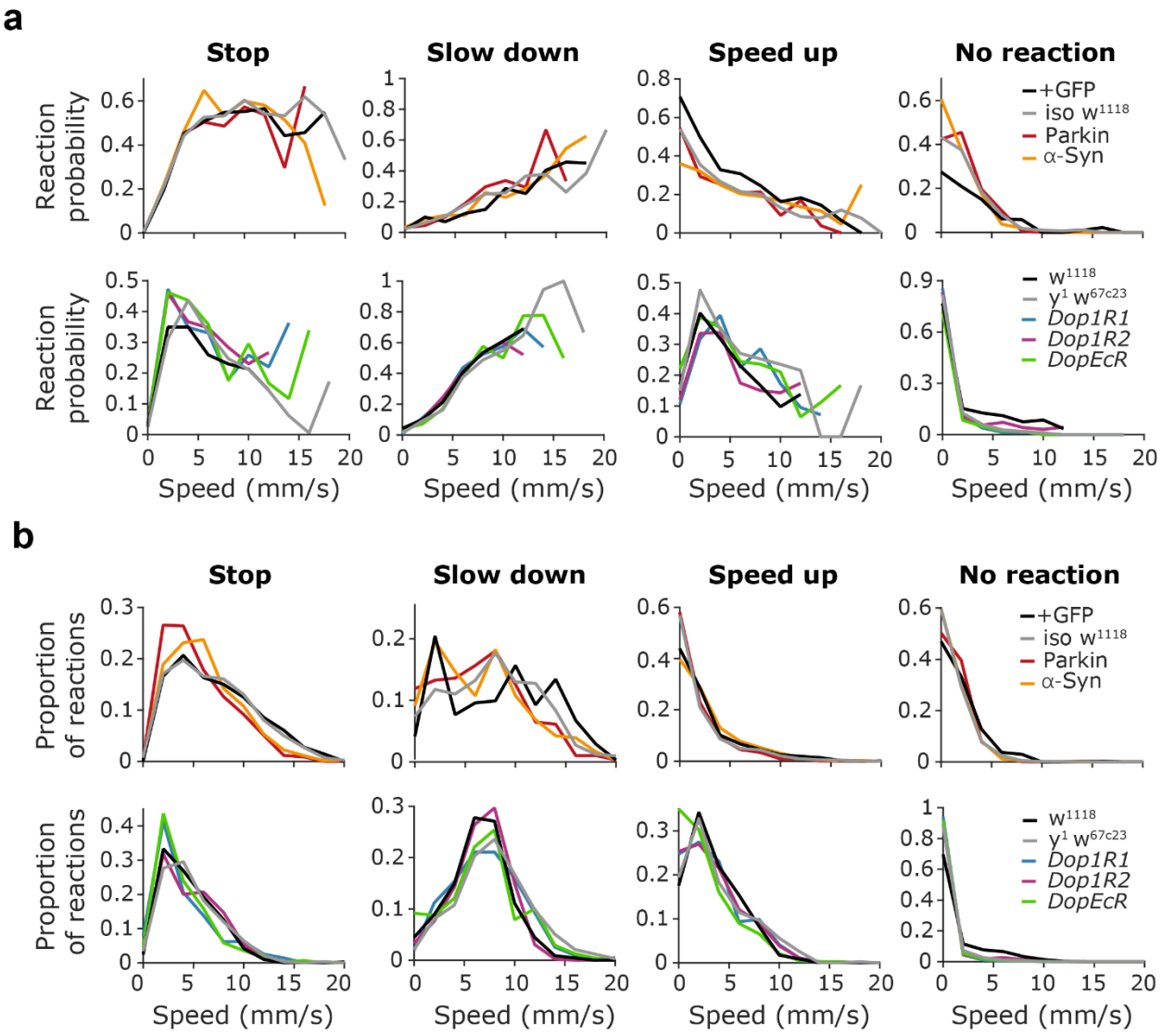

629

630

Figure 5

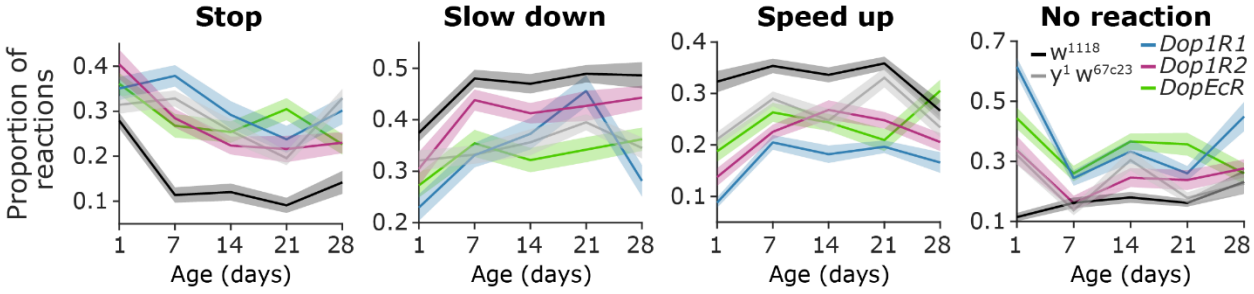
Stop
Slow down
Speed up
No reaction
Proportion of reactions
Age (days)
w1118
y1 w67c23
Dop1R1
Dop1R2
DopEcR

Supplementary Figures

Figure S1

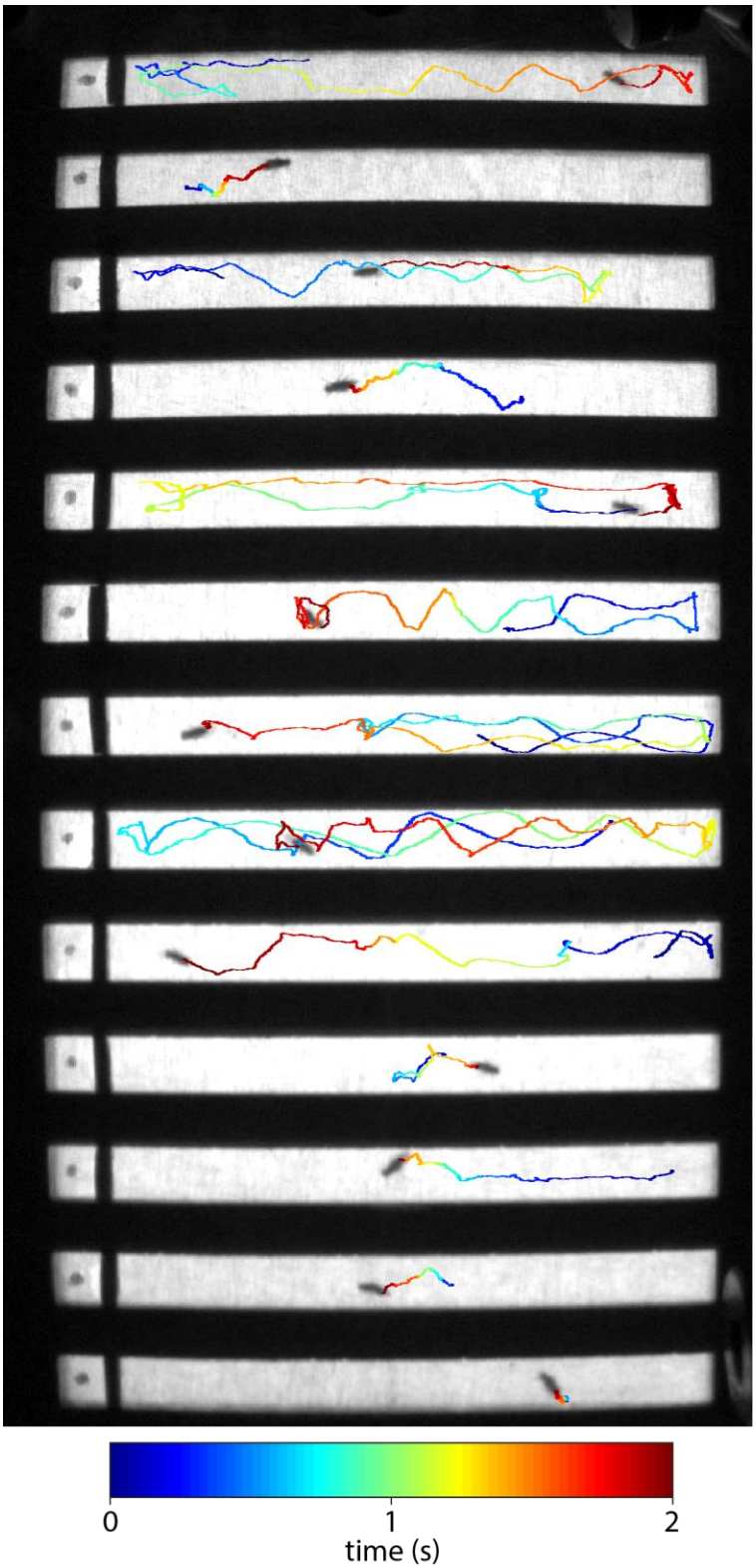

Figure S2

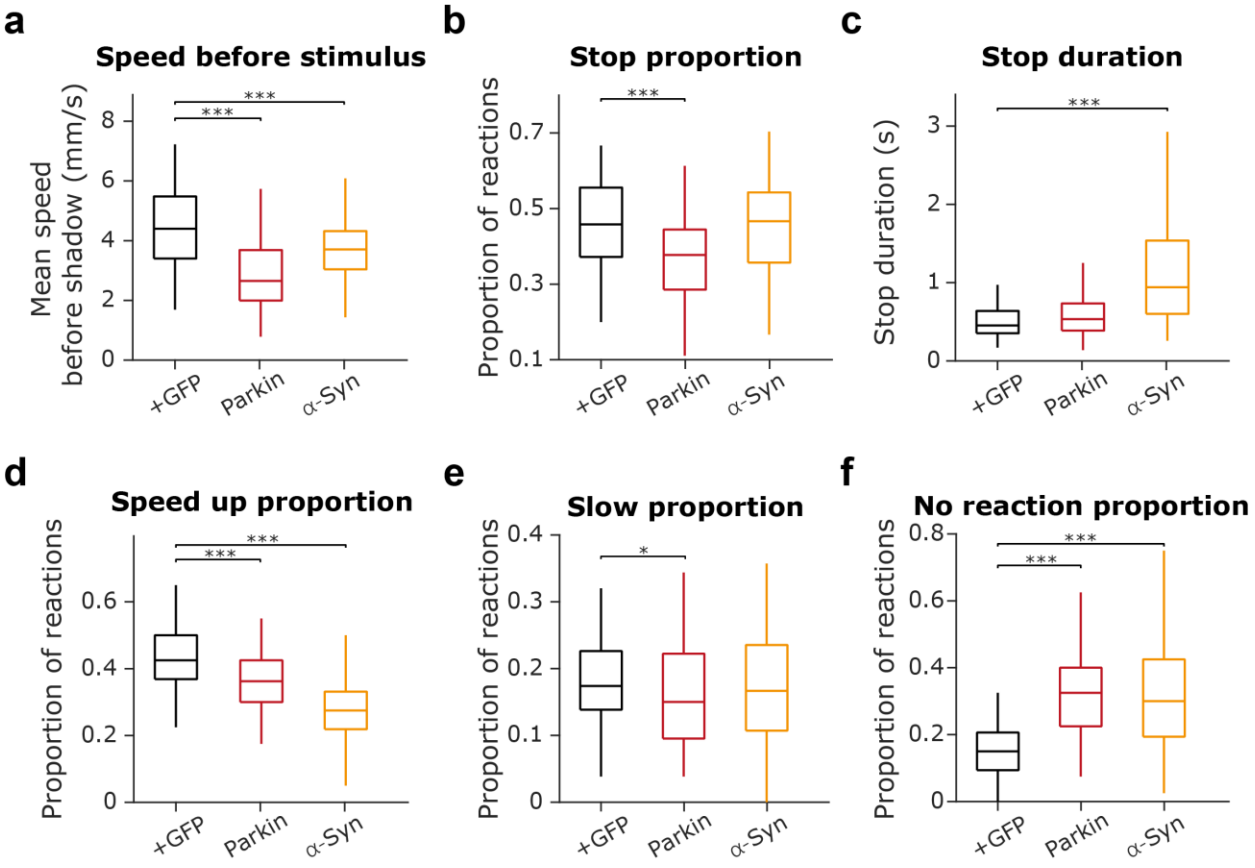
a
Speed before stimulus
Mean speed before shadow (mm/s)
0
2
4
6
8
***
***
+GFP
Parkin
α-Syn
b
Stop proportion
Proportion of reactions
0.1
0.3
0.5
0.7
***
+GFP
Parkin
α-Syn
c
Stop duration
Stop duration (s)
0
1
2
3
***
+GFP
Parkin
α-Syn
d
Speed up proportion
Proportion of reactions
0
0.2
0.4
0.6
***
***
+GFP
Parkin
α-Syn
e
Slow proportion
Proportion of reactions
0
0.1
0.2
0.3
0.4
*
+GFP
Parkin
α-Syn
f
No reaction proportion
Proportion of reactions
0
0.2
0.4
0.6
0.8
***
***
+GFP
Parkin
α-Syn

640 **Figure S3**

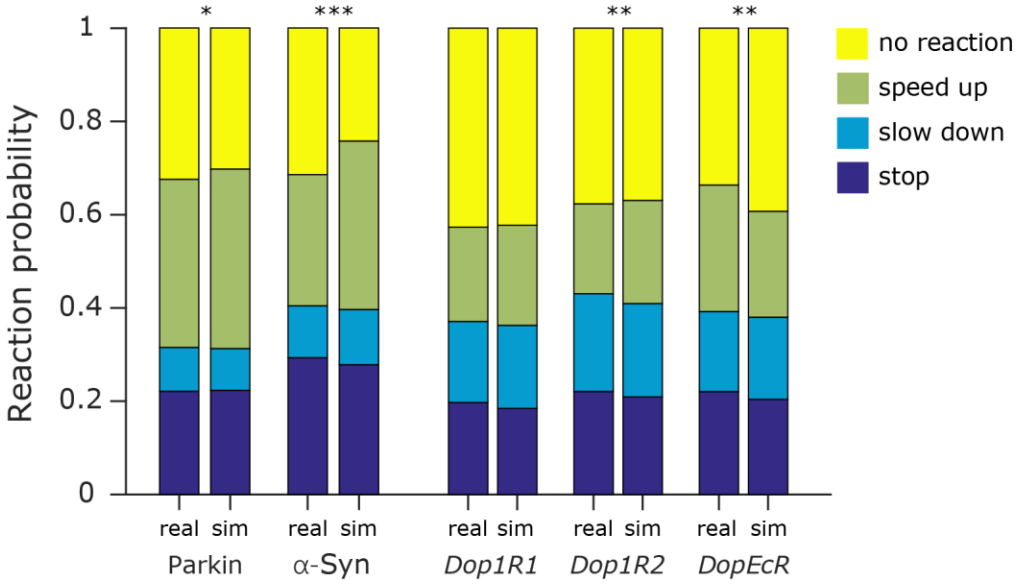

641

642

Figure S4

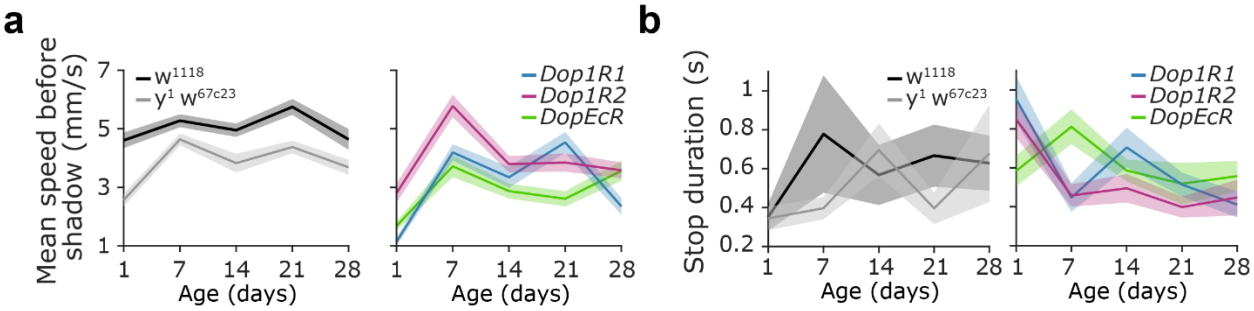
a
Mean speed before shadow (mm/s)
7
5
3
1
w1118
y1 w67c23
1 7 14 21 28
Age (days)
Dop1R1
Dop1R2
DopEcR
1 7 14 21 28
Age (days)
b
Stop duration (s)
1
0.8
0.6
0.4
0.2
w1118
y1 w67c23
1 7 14 21 28
Age (days)
Dop1R1
Dop1R2
DopEcR
1 7 14 21 28
Age (days)